Available online at www.sciencedirect.com
SCIENCE DIRECT®
Scripta Materialia 50 (2004) 1085–1090
Scripta MATERIALIA
www.actamat-journals.com

Study on the orientational stability of cube-oriented FCC crystals under plane strain by use of a texture component crystal plasticity finite element method

D. Raabe [a,*], Z. Zhao [b], F. Roters [a]

[a] Max-Planck-Institut für Eisenforschung, Microstructure Physics, Max-Planck-Str. 1, 40237 Düsseldorf, Germany
[b] Department of Aeronautics and Astronautics, Massachusetts Institute of Technology, 77 Massachusetts Avenue, Cambridge, MA 02139, USA

Received 4 April 2003; received in revised form 5 November 2003; accepted 29 November 2003

Abstract

We study orientational grain fragmentation of cube-oriented FCC crystals by using a texture component based crystal plasticity finite element method. We describe the starting texture of the crystals in terms of a spherical Gaussian. Orientational in-grain heterogeneity occurring during loading is investigated as a function of friction and orientation scatter.

Keywords: Texture; Modeling; Structural behavior; Mechanical properties; Plasticity; Crystalline; Mesostructure

1. Motivation for this study

Cube-oriented face centered cubic (FCC) crystals exhibit the evolution of heterogeneous in-grain crystallographic microtextures and deformation structures during plane strain compression [1–15]. Cube-oriented FCC crystals are *metastable* under plane strain, i.e. upon loading they can show lattice rotations about the normal direction (ND), the rolling direction (RD), or transverse direction (TD) depending on the initial orientation spread prior to loading and on the mechanical boundary conditions.

Many experiments have documented the dependence and the sensitivity of the microtexture and microstructure evolution in cube crystals on the deformation conditions [1–15]. In these studies it was observed that due to the kinematical metastability of the cube orientation small changes in boundary conditions may entail significant changes in microstructure and texture.

Various models were suggested to predict the microtextures of cube-oriented FCC crystals during deformation which, however, in part contradict each other. For example, early models for in-grain lattice rotations about ND and RD were suggested by Dillamore and Katoh [16] as well as by Lee et al. [17]. Other models favoring rotations about TD were later suggested by the groups of Hansen [7] and Driver [11].

From this concise introduction to the field we can extract two main aspects of microtexture evolution in cube-oriented grains. First, no model has been able so far to cover all experimental observations of lattice re-orientations made by the various groups [1–15]. In particular, it is unclear whether the intrinsic re-orientation tendency of cube crystals under plane strain loading leads to rotations about TD, ND, or RD. Second, the behavior of single cube crystals under plane strain loads is obviously sensitive to the mechanical boundary conditions. Both aspects imply that a refined model which aims at explaining these observations must be sufficiently sensitive with respect to small variations in starting and boundary conditions (e.g. initial small texture variation within the cube grain or changes in friction).

2. Theoretical approach

2.1. Introduction to the texture-component crystal plasticity finite element method

Strong progress in the field of texture modeling has been made by the introduction of crystal plasticity finite

* Corresponding author. Tel.: +49-211-679-2278; fax: +49-211-679-2333.
E-mail address: raabe@mpie.de (D. Raabe).

1359-6462/$ - see front matter © 2003 Acta Materialia Inc. Published by Elsevier Ltd. All rights reserved.
doi:10.1016/j.scriptamat.2003.11.061

element methods [18–23]. Their particular strength lies in the application of realistic mechanical boundary conditions to fairly realistic initial microstructures. This enables the user to take into account both, details of the external loading and of the internal crystalline constitutive response at the same time. In our study we use this approach as a basis for the formulation of a novel texture component crystal plasticity finite element model [24] which we then apply to the investigation of the influence of starting and boundary conditions on the deformation of cube-oriented FCC crystals.

The key idea of our new model variant lies in identifying a method of mapping a *representative* crystallographic orientation distribution, comprising a *huge* number of crystal portions, on the Gauss points of a finite element mesh using a compact mathematical form. For this purpose we use the orientation component method [25,26] which is a technique of approximating an orientation distribution function in the form of one or more symmetrical spherical central standard functions. Such standard functions [25–28] have individual height and full width at half maximum as a measure for the strength and scatter of the crystallographic component they represent. The novelty of our approach lies in the connection of orientation components to a suited crystal elasticity and plasticity constitutive model (we use the formulation of Kalidindi [20]). The task of the approach is to represent (in the present case) one spherical orientation component (namely, the cube) on the integration points of a finite element mesh. This procedure works in two steps: In the first step the discrete orientation g^c (center of the Gauss distribution) is defined for an orientation component and assigned in terms of its respective Euler triple $(\varphi_1, \phi, \varphi_2)$, i.e. in the form of a *single* rotation matrix, onto *each* integration point (Fig. 1). In the second step, these discrete orientations are re-oriented in such a fashion that their resulting distribution reproduces the Gauss function originally prescribed (Fig. 1). This means that the scatter which was originally only given in orientation space is now represented by a distribution both, in real space and in orientation space.

After this mapping procedure, the texture component concept is no longer required. This is due to the fact that during the subsequent simulation each individual orientation portion originally pertaining to a common component can undergo an *individual* orientation change. This means that the orientation component method is used to *feed* a crystallographic orientation distribution into a finite element simulation on a strictly scaleable and quantitative basis, but the components are in their original form not tracked during the simulation.

2.2. Model assembly

Fig. 2 shows the assembly of the finite element model. Four surfaces were used to describe the boundary conditions for the simulated plane strain compression tests. This geometry and individual surface treatment was chosen to mimic macroscopic boundary conditions typical of a channel die experiment. The sample consisted of 500 three-dimensional linear elements each with eight integration points. An implicit crystal plasticity procedure proposed by Kalidindi [20] was implemented and used for the time integration of the constitutive equations. The simulations used $\{1\,1\,1\}\langle 1\,1\,0\rangle$ slip systems and viscoplastic hardening. Different friction coefficients (linear Coulomb law) were used to investigate the influence of shear. All simulations were conducted to 50% engineering thickness reduction.

3. Results and discussion

3.1. Orientational stability of an ideal cube single crystal

Fig. 3 shows the simulation results obtained for the plane strain compression of an initially *exactly* cube oriented and perfectly homogeneous single crystal, i.e. all elements had the *same* initial orientation $\varphi_1 = 0°$, $\phi = 0°$, $\varphi_2 = 0°$ without any initial orientation scatter). The friction coefficients on the top surface (contact surface with compression plane) and bottom surface (surfaces 1 and 2 in Fig. 2) were $\mu = 0.1$. The friction

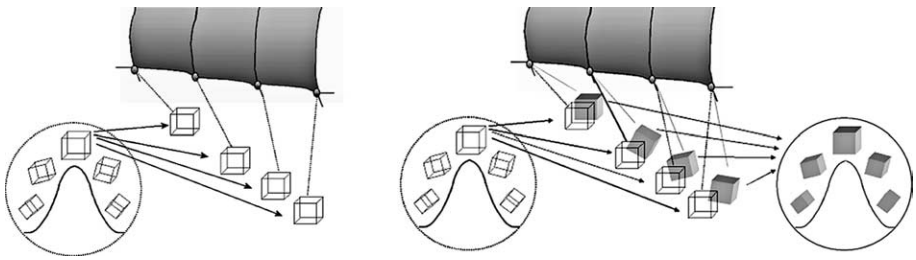

Fig. 1. The decomposition of a cube-oriented spherical component consists in extracting the preferred orientation from the function (i.e. $\varphi_1 = 0°$, $\phi = 0°$, $\varphi_2 = 0°$ for cube, Bunge-Euler notation) and assigning it in the form of a single rotation matrix onto each integration point (left hand side). In the second step (right hand side) all orientation portions, defined by the integration points, are re-oriented to reproduce the prescribed orientation distribution.

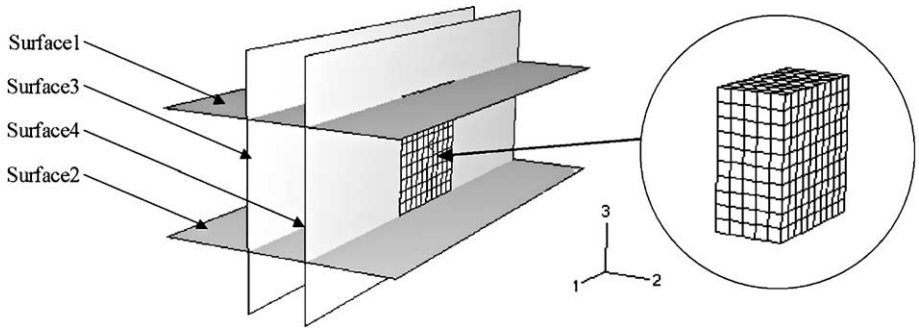

Fig. 2. Setup of the finite element model (500 3D linear elements). Four rigid surfaces were used to simulate the boundary conditions during plane strain compression, in particular different friction conditions of the different surfaces.

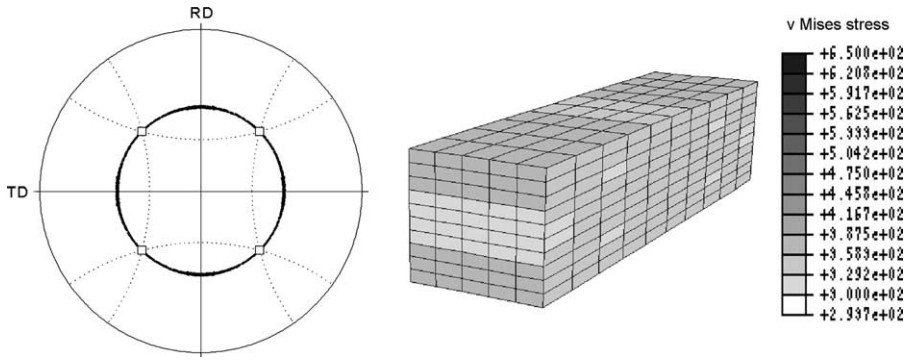

Fig. 3. Simulation result for plane strain compression of a cube single crystal. An exact cube orientation ($\varphi_1 = 0°$, $\phi = 0°$, $\varphi_2 = 0°$) without any initial orientation scatter was assigned to all elements prior to loading. The friction coefficient on surfaces 1 and 2 was $\mu = 0.1$. The sample was 50% reduced in thickness (engineering strain measure).

coefficients on the two side surfaces were zero. Fig. 3 shows that the elements preserved a regular brick-like shape after 50% deformation (engineering strain measure). The gray scale color code describes the von Mises stress. It is very homogeneous throughout the specimen. The {1 1 1} pole figure shows that orientational splitting occurred only about ND. The orientation scatter is very symmetric.

3.2. Orientational stability of a cube single crystal with Gaussian orientation scatter

As-grown single crystals are never perfect but contain lattice defects prior to loading, i.e. the orientation distribution in single crystals is neither a delta function in orientation space nor laterally constant. The microtexture in a real single crystal can, therefore, be described in the form of an *ideal* (or *exact*) orientation together with an orientational scatter around it. In the framework of the texture component method introduced above we describe the starting texture of the cube single crystal in the form of a spherical Gauss component with a full width at half maximum of 2.5°. This means that we map a set of single orientations onto the finite element mesh which satisfies a spherical Gaussian central function about the ideal cube orientation (Fig. 4). The 500 discrete orientations were assigned in random lateral order to the elements of the finite element mesh.

Fig. 5 shows the deformation results for this set-up. The other simulation parameters were identical to those used in Section 3.1. In clear difference to the results for the perfect initial cube orientation (Fig. 3) the pole figure in Fig. 5 shows that orientation splitting occurs about ND and RD. Fig. 8a shows the corresponding section from the orientation distribution function (ODF). It clearly reveals that the orientation spread after deformation is larger about RD ($\sim$22° for $f(g) = 10$) than about ND ($\sim$14° for $f(g) = 10$). It must be noted in this context that the data which are exactly located on one of the two axes correspond to pure RD or respectively ND rotations. The finite element mesh and the stress distribution shows that slight shear distortion occurred in most elements.

3.3. Orientational stability of a cube single crystal with Gaussian orientation scatter under large-friction conditions

Fig. 6 shows the simulation results for the same case as presented in Fig. 5, but the friction coefficient

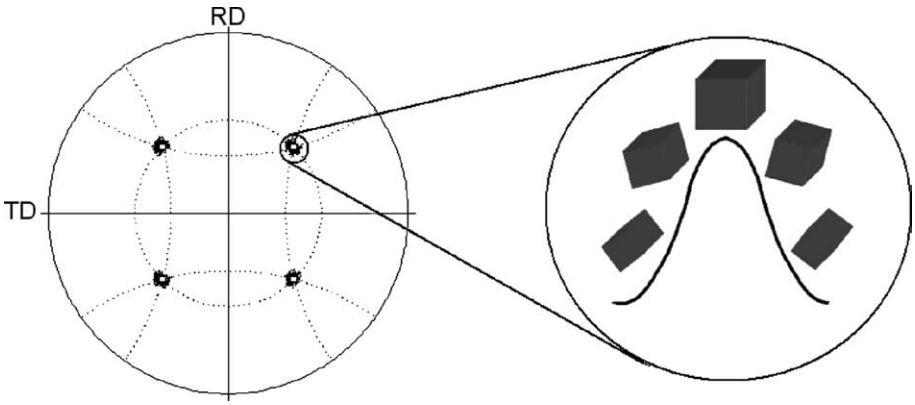

Fig. 4. Gauss-type spherical approximation of the initial microtexture within a cube single crystal consisting of 500 single orientations in a stereographic {1 1 1} pole figure projection. The full width at half maximum amounts to 2.5°.

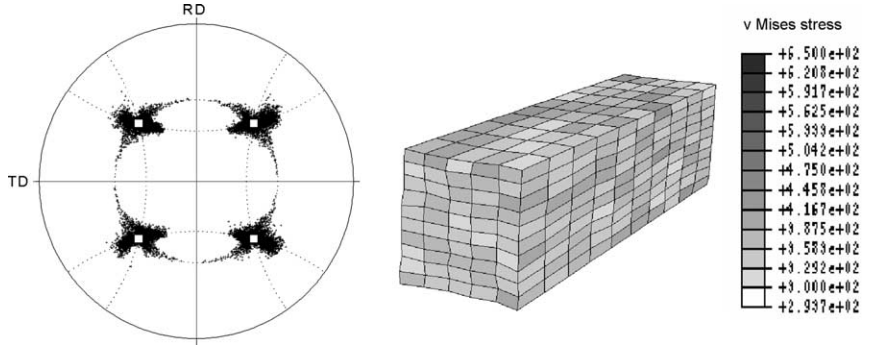

Fig. 5. Simulation results for plane strain compression of a single crystal with a 2.5° spherical Gaussian orientation scatter about the exact cube orientation prior to loading. Friction occurs only on surfaces 1 and 2 (top and bottom) with a friction coefficient of $\mu = 0.1$. See also the ODF section in Fig. 8.

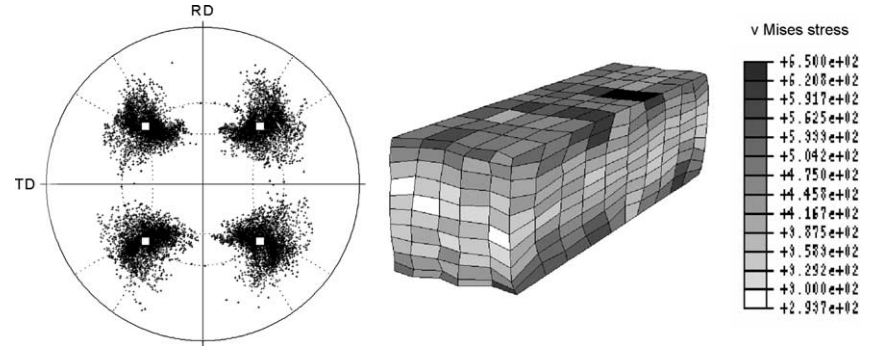

Fig. 6. Simulation results for plane strain compression of a single crystal with a 2.5° spherical Gaussian orientation scatter about the exact cube orientation prior to loading. Friction only occurs on surfaces 1 and 2 (top and bottom) with a friction coefficient of $\mu = 0.3$. See also the ODF section in Fig. 8.

amounted to $\mu = 0.3$. All other parameters were the same as in Fig. 5. Orientation splitting during forming clearly increases with larger friction on the top and bottom surfaces. Although the re-orientation behavior of most elements is similar to that shown in Fig. 5 additional orientation scatter appears about TD. The scatter about the ND axis (Fig. 8b) is smaller than that for the data shown in Figs. 5 and 8a. It is also important to note that the overall orientational scatter in Fig. 6 is more smeared out than that for the case with smaller

friction (Fig. 5). This is also shown by the ODF which reveals a much smaller maximum in the orientation density at the exact cube component (Fig. 8b) when compared to that for the case shown in Fig. 8a. Another difference to Fig. 5 is that Fig. 6 shows more pronounced element distortion and a more inhomogeneous stress distribution.

3.4. Orientational stability of a cube single crystal with Gaussian orientation scatter under surround friction conditions

Fig. 7 shows the simulation results obtained for plane strain compression of a cube single crystal with an initial Gaussian orientation scatter of 2.5° assuming a friction coefficient of $\mu = 0.1$ on all four longitudinal surfaces (see surfaces 1–4 in Fig. 2). The other simulation parameters were the same as in Figs. 5 and 6. The orientational scatter shows a strong component about TD together with some weaker ND and RD scatter (Fig. 8c). Particularly the RD scatter is smaller than that for the simulation with non-zero friction on only two surfaces (Figs. 5 and 8a).

3.5. Influence of initial orientation scatter and of friction on the re-orientation behavior of cube crystals

Comparison of the results for an *ideal* initial cube texture (Fig. 3) and for an initial Gaussian orientation scatter (Figs. 4, 5) for *identical* friction conditions reveals that the simulation method is sufficiently sensitive to account for effects arising from fine changes in starting texture. The texture in Fig. 5 is characterized by strong orientation splitting not only about ND, like in Fig. 3, but even more pronounced about RD (Fig. 8a).

These results confirm many experiments [7–11], namely, that the cube orientation is metastable under plane strain conditions. This was also found in recent theoretical studies on the re-orientation behavior of different orientations by use of homogenization and crystal plasticity finite element analysis [29,30]. This investigation also confirmed that orientation gradients in initially uniform cube crystals can occur under gradient-free external loads. The intrinsic origin of this effect was quantified in terms of the change in crystal re-orientation upon small changes in initial orientation. Such starting conditions are in the present study

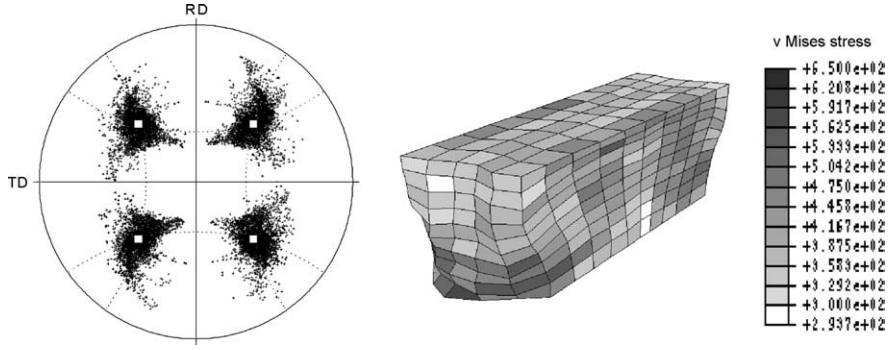

Fig. 7. Simulation results for plane strain compression of a single crystal with a 2.5° spherical Gaussian orientation scatter about the exact cube orientation prior to loading. Friction occurs on four surfaces with a friction coefficient of $\mu = 0.1$. See also the ODF section in Fig. 8.

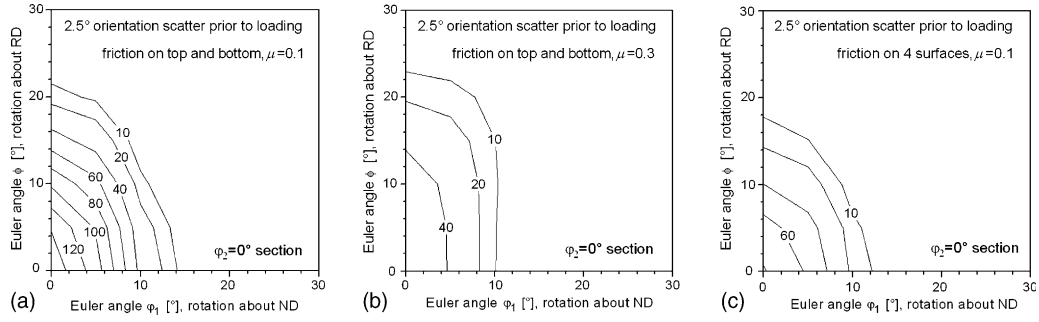

Fig. 8. Quantitative presentation of the in-grain orientation spread resulting after deformation in terms of $\varphi_2 = 0°$ sections from the orientation distribution function (ODF) for the three examples given in Figs. 5–7 in terms of pole figures (ND: normal direction; RD: rolling direction). The data which are exactly located on one of the two axes correspond to pure RD or respectively ND rotations. (a) 2.5° Orientation scatter prior to loading, friction on top and bottom, $\mu = 0.1$ (see Fig. 5); (b) 2.5° orientation scatter prior to loading, friction on top and bottom, $\mu = 0.3$ (see Fig. 6); (c) 2.5° orientation scatter prior to loading, friction on four surfaces, $\mu = 0.1$ (see Fig. 7).

represented by the Gaussian orientation scatter prior to deformation. The theory in [29,30] was formulated as a divergence operator applied to re-orientation rate vector fields. The obtained scalar divergence function gave an excellent quantification of the stability of grains under homogeneous boundary conditions as a function of their orientation. Positive divergence which is a source in the re-orientation rate vector field characterize orientations with diverging non-zero reorientation rates which are kinematically instable and prone to build up orientation gradients.

Besides such basic kinematical interpretation we attribute the deviation between Figs. 3 and 5 also in terms of the loss in *local* symmetry (Fig. 5). The slight element distortion shows that due to the laterally random distribution of the imposed initial 2.5° orientation scatter the plane strain state is locally violated entailing strong RD rotations (Fig. 8). These observations correspond to a recent study [31] which showed that weakly positive divergent orientations, such as cube in FCC, reveal a larger dependence of their re-orientation behavior on the local mechanical boundary conditions (local deviation from a plane strain state) and, therefore, a larger variety of the resulting orientation spreads, than less divergent crystals [29,30].

Such effects arising from the loss in local symmetry are surely assisted by friction. However, the influence of friction is likely to promote TD rotations rather than RD rotations because it induces longitudinal shear strains [32]. With increasing friction coefficient and increasing number of surfaces imposing non-zero friction (Fig. 6), the orientation and stress distribution becomes increasingly heterogeneous. The differences between Figs. 5 and 6 which originate from an increase in the friction coefficient from $\mu = 0.1$ (Fig. 5) to $\mu = 0.3$ (Fig. 6) clearly show that particularly strong forward shears lead to TD rotations. Samples which are plane strain deformed with small friction (Figs. 3 and 5) reveal mainly ND or RD re-orientations depending on the initial orientation scatter (Fig. 8).

4. Conclusions

We investigated the orientational stability of cube FCC crystals under plane strain (50% engineering thickness reduction) by use of a texture component crystal plasticity finite element method. The main results are:

- If the friction is small ($\mu = 0.1$) and the initial orientation of the sample is *exactly* cube everywhere in the mesh (all elements have the *same* initial orientation $\varphi_1 = 0°$, $\phi = 0°$, $\varphi_2 = 0°$ without any initial orientation scatter prior to loading) the orientation spread after deformation can be described in terms of a pure ND rotation.
- If the friction is small ($\mu = 0.1$) and the initial orientation of the sample is a cube orientation with 2.5° spherical Gaussian scatter the orientation spread after deformation can be described in terms of ND *and* RD rotations.
- If the friction is large ($\mu = 0.3$) and the initial orientation of the sample is a cube orientation with 2.5° spherical Gaussian scatter the orientation spread after deformation can be described in terms of ND, RD, *and* TD rotations. The latter rotation mode is due to the induced forward shear.

References

[1] Dahl O, Pawlek F. Z Metallk 1936;72:310.
[2] Malin A, Huber J, Hatherly M. Z Metallk 1981;72:310.
[3] Norestad L, Oscarsson A, Hutchinson WB. Scripta Met 1987;21:491.
[4] Daaland O, Nes E. Acta Mater 1996;44:1389.
[5] Sindel M, Köhlhoff GD, Lücke K, Duggan BJ. Text Microstruc 1990;12:37.
[6] Vatne HE, Shahani R, Nes E. Acta Mater 1996;44:4447.
[7] Wert JA, Liu Q, Hansen N. Acta Mater 1997;45:2565.
[8] Hansen N, Huang X. Acta Mater 1998;46:1827.
[9] Liu Q, Maurice C, Driver JH, Hansen N. Metall Mater Trans 1998;29A:2333.
[10] Maurice C, Driver JH. Acta Mater 1997;45:4627.
[11] Basson F, Driver JH. Acta Metall 2000;48:2101.
[12] Huang Y, Humphreys FJ, Ferry M. Acta Metall 2000;48:2543.
[13] Zaefferer S, Baudin T, Penelle R. Acta Metall 2001;49:1105.
[14] Wert JA. Acta Mater 2002;50:3125.
[15] Stanford N, Dunne D, Ferry M. Mater Sci Eng, in press.
[16] Dillamore L, Katoh H. Metals Sci 1974;8:73.
[17] Lee CS, Duggan BJ, Smallman RE. Acta Metall 1993;41:2265.
[18] Dève H, Harren SV, McCullough C, Asaro RJ. Acta Metall 1988;36:341.
[19] Becker RC. Acta Metall 1991;39:1211.
[20] Kalidindi SR, Bronkhorst CA, Anand L. J Mech Phys Solids 1992;40:537.
[21] Dawson PR, Beaudoin AJ, Mathur KK. In: Andersen SI, Bilde-Sørensen JB, Lorentzen T, Pedersen OB, Sorensen NJ, editors. Proceedings of 15th RISØ Internnational Symposium Materials Science, RISØ National Laboratory, Roskilde, Denmark, 1994. p. 33.
[22] Beaudoin J, Mecking H, Kocks UF. Philos Mag A 1996;73:1503.
[23] Raabe D, Sachtleber M, Zhao Z, Roters F, Zaefferer S. Acta Mater 2001;49:3433.
[24] Raabe D, Roters F. Int J Plasticity 2004;20:339–61.
[25] Lücke K, Pospiech J, Virnich KH, Jura J. Acta Metall 1981;29:167.
[26] Helming K, Schwarzer RA, Rauschenbach B, Geier S, Leiss B, Wenk HR, et al. Z Metall 1994;85:545.
[27] Raabe D, Lücke K. Mater Sci Forum 1994;157–162:413.
[28] Raabe D, Lücke K. Phys Stat Sol (b) 1993;180:59.
[29] Raabe D, Zhao Z, Roters F. Proceedings 13th International Conference Textures of Materials. In: Lee DN, editor. Materials Science Forum, vol. 408–412, 2002, p. 275.
[30] Raabe D, Zhao Z, Park SJ, Roters F. Acta Mater 2002;50:421.
[31] Raabe D, Zhao Z, Mao W. Acta Mater 2002;50:4379.
[32] Hölscher M, Raabe D, Lücke K. Acta Metall 1994;42:879.